Engineered Science
DOI: https://dx.doi.org/10.30919/es912

Analyzing Two Laser Thermal Energy Calculation Equations: A Comparison of Beer-Lambert's Law and Light Transport Equation

Jedsadakorn Saemathong, Nattadon Pannucharoenwong,* Vannakorn Mongkol, Somsak Vongpradubchai and Phadungsak Rattanadecho

Abstract

An estimated 2-3 million skin cancers are occurring worldwide each year, most of which are caused by UV exposure. Therefore, many methods of prevention and treatment are required. As a result, a new technique for treatment, such as the use of laser treatment, has been proposed to study through mathematical models because human studies have ethical limitations. Previously, the laser power was calculated using two of the most widely used laser equations: Beer-lambert's law (BLL) and light transport equation (LTE). In this work, the temperature distribution from the two equations was studied and compared, and the effect of skin thickness is also being investigated. The study found that in the model, the thickness of the thin epidermis at low wavelengths was slightly different and interchangeable. However, the Light Transport Equation model has a higher depth temperature distribution at high wavelengths 800 and 980 nm in thin and thick models. There was a clear difference in temperature distribution in the simulations exposed to high-wavelength laser radiation. Furthermore, the laser beam radius and fluency rate impact the temperature distribution in the same way, i.e., as the calculated model temperature parameter increases. The radial temperature distribution increases as the laser beam radius increases.

Keywords: Light transport equation; Laser energy; Mathematical models; Temperature distribution.
Received: 03 April 2023; Revised: 16 June 2023; Accepted: 18 June 2023.
Article type: Research article.

1. Introduction

Since the 1960s, lasers have been around for a long time.[1] They have been employed in industry since the nineteenth century[2] and are now widely used in treatment.[3] This necessitates a variety of considerations. The medical laser uses include hair removal, dermatology, and others. It is applied to treat a wide range of skin conditions, including Rosacea, a chronic skin condition of the face or eyes in women, and hair removal.[4,5]

A new concept for the use of lasers to treat skin malignancies induced by excessive exposure to ultraviolet radiation during infancy and adolescence has been developed.[6,7] Laser treatment has a shortened healing time, a smaller incision size, and no chemical side effects such as hair loss, nausea or vomiting, fatigue, irritation of the mucous membranes or mouth, and diarrhea when compared to conventional treatments such as surgery and chemotherapy.[8] When the laser is applied to the epidermis, thermal energy is produced. Extreme heat can cause injury, so it is necessary to ascertain the extent of treatment. However, ethical constraints make human research impractical. Consequently, a mathematical model study is an intriguing alternative research method. A mathematical equation is utilized to calculate the energy absorbed and converted to heat because the patient's body has diverse characteristics, such as skin tones, humidity, and treatment outcomes.[9,10] Therefore, scientific and engineering knowledge is necessary to ascertain the extent of treatment.

Pennes developed a biological tissue model for estimating dermal heat transfer in order to investigate the effect of blood flow on heat transmission in biological tissues. The generated

Center of Excellence in Electromagnetic Energy Utilization in Engineering (CEEE), Department of Mechanical Engineering, Faculty of Engineering, Thammasat School of Engineering, Thammasat University, 12120, Thailand.
**Email:* pnattado@engr.tu.ac.th (N. Pannucharoenwong)

model will be a useful tool for future research and experimentation on the effects of external heat sources on the skin.[11] The Pennes biothermal model was utilized in research such as by Jaunich *et al*. (2008). Using a non-Fourier-Pennes bioheat transfer model and a brief pulse laser irradiation, the temperature distribution in inhomogeneities of a multilayer simulated embedded tissue model was investigated.[12] In 2015, Bhowmik *et al*. published a study on breast cancers using the Pennes bioheat heat transfer equation and laser thermal energy.[13]

Several studies have been conducted into mathematical models in which external thermal energy is produced from a laser using Beer-Lambert's law, including Jauch *et al*.'s 2008 study. In addition, Kim *et al*. created a numerical thermal model based on skin at various wavelengths and conducted experiments for four distinct laser wavelengths in order to investigate differences in temperature distribution for each skin type in the hair removal model 2014[14] Other studies have examined a mathematical model of biothermal energy caused by laser external thermal energy as calculated by Beer-Lambert's Law.[15-17]

Additionally, the Beer-Lambert law is employed to calculate the external energy of biological heat transfer. Another well-known equation, the light transport equation, is used to analyze mathematical models for laser treatment procedures such as hair removal, cancer therapy, and others. This is the equation characterizing the medium's light transmission.[18] For example, Shafirstien *et al*. investigated and validated the propagation estimation theory in 2004 to identify optimal laser wavelengths and radiation exposures for the treatment of port-wine stains.[19] The light transport equation has been used to calculate other studies on external heat energy.[20-22]

The model presented in Table 1 estimates the external

Table 1. Literature review summary.

Author (year)	Research Area	External Heat Source		Method	
		BLL	LTE	Sim	Exp
Shafirstien *et al.*, (2004)	Light-tissue simulations were studied and analytical methods for diffusion estimation theory were used to find the best laser wavelength and radiation exposure for treating port-wine stains (PWS)		✓	✓	
Zhang *et al.*, (2005)	Comparison of diffusion estimates and finite element models based on Monte Carlo for modeling the laser-induced heat response in discrete vessels Using a model, the distribution of light in a multilayered human epidermis with or without discrete veins was studied.		✓	✓	
Juanich *et al.*, (2008)	Bio-heat transfer study during tissue irradiation with a short pulse laser.	✓		✓	✓
Kim *et al.*, (2014)	In order to construct a numerical thermal model based on skin conditions at different wavelengths, four distinct wavelength diode lasers were used experimentally on two separate hair removal skin models.	✓		✓	✓
Bhowmik *et al.*, (2015)	Evaporated ultrasound and laser heating models for breast malignancies were studied.	✓		✓	
Wongchadakul *et al*., (2018)	Study the different components of lasers that affect heat transfer and tissue shrinkage.	✓		✓	
Wongchadakul *et al*., (2019)	The investigation of alterations in human epidermis varieties exposed to distinct laser wavelengths	✓		✓	
Paul *et al*., (2021)	Examine the thermomechanical response of vascular tissues with and without nanoparticles for the following heating modes: continuous, pulse, interstitial laser heating, and focused ultrasound.		✓	✓	✓
Wongchadakul et al., (2021)	In a mathematical model with a multilayered epidermis and an embedded tumor, the impact of coupling laser ablation and nanoparticles was investigated.	✓		✓	

BLL = Beer-lambert's law, LTE = Light transport equation, Sim = Simulation, and Exp = Experimental

energy of a laser by utilizing two modes. The transport equation and Beer-Lambert's law According to the data, the majority of previous laser energy investigations were founded on both equations. In addition, the two equations have little in common regarding horticulture. This study examined the difference between the two equations following laser thermal therapy. Due to the disparities between the two equations, little research has been conducted on the effect of laser irradiation on epidermal thickness to facilitate the adaptation of each study to the model, where applicable. Therefore, we analyzed the influence of epidermal thickness on temperature distribution. It has multiple applications for diverse investigations.

The effect of thermal vibration on the analysis of nonhomogeneous nanobeams has been demonstrated in previous research.[23,24] Consequently, it is conceivable that the heterogeneity influenced the model's heterogeneity. Erfan Salari's model of porous nanomaterial sheets or beams was subsequently examined. *et al.*, who investigated the thermal deflection of non-homogeneous nanosheets, found that the thermal deflection varied with the direction of thickness and was determined by a power law function.[25,26] as well as to investigate the microscopic material scale and the heterogeneity of the material that affects temperature.[27,28] The two characteristics of porosity distribution influence the dynamic snap-through deflection and vibration characteristics of functionally graded nanobeams following deflection.[29] After thermal deflection and nonlinear thermal bending of the nanobeams, the geometric imperfections of the nanobeams were also considered.[30] In future investigations, the theory of porous materials will be employed to analyze the behavior of heterogeneous tissues based on previous research.

2. Modelling

The biological structure is composed of 3 layers of tissues: epidermis, dermis, and hypodermis. It is a domain that determines the temperature in tissues when treated with laser energy from the temperature distribution. In this work, an axial symmetrical 2D model was created utilizing laser irradiation with Beer-lambert's law and Light transport equation. The phenomena were based on the parameters presented in Table 2.

Table 2. Optical properties, thermal properties and physical properties.[13,33-36]

Parameter	Epidermis	Dermis	Hypodermis
Thickness (Thick/Slim) [mm]	0.05/1.50	1.95/1.50	10/9
Tissue density, ρ [kg/m^3]	1200	1200	1000
Specific heat of tissue, c [J/kg.K]	3600	3800	3600
Thermal conductivity, k [W/(m.K)]	0.21	0.53	0.55
Blood perfusion, w_b [1/s]	0	0.0031	0.0031
Metabolic heat generation, Q_{met} [W/m^3]	368	368	368
Absorption coefficient, μ_a [1/m], 694 nm	2277	29	127
Absorption coefficient, μ_a [1/m], 800 nm	1418	26	108
Absorption coefficient, μ_a [1/m], 980 nm	720	25.5	89
Scattering coefficient, μ_s [1/m], 694 nm	1956	1956	23000
Scattering coefficient, μ_s [1/m], 800 nm	1372	1372	20200
Scattering coefficient, μ_s [1/m], 980 nm	732	732	17400
Optical anisotropy factor, 694 nm	0.9	0.79	0.9
Optical anisotropy factor, 800 nm	0.85	0.85	0.85
Optical anisotropy factor, 980 nm	0.85	0.85	0.85
Reflectance	0.65	0.6	0.5
The width of the irradiated area, σ [mm]	1,2		
Ambient temperature, T_{am} [°C]	25		
Initial temperature, T_0 [°C]	37		
Blood temperature, T_b [°C]	37		
Heat convection coefficient, h [W/m^2.K]	20		
Blood density, ρ_b [kg/m^3]	1060		
Specific heat of blood, c_b [J/kg.K]	3660		
Speed of light in tissue, c_* [m/s]	2.19×10^8		
Fluent rate, f [J/cm^2]	50, 100		
Power, P [W/m^2]	Fluent rate/time		

2.1 Problem description

Laser irradiation is the application of light at various wavelengths to a target to create heat using Pennes' Bioheat Equation. For each wavelength, the laser's external thermal energy is computed using Beer-lambert's law and Light transport equation (694 nm, 800 nm, and 980 nm). Optical characteristics differ depending on wavelength. This treatment objective is to cure skin cancer while preserving healthy tissue around it.

The epidermis, dermis, and hypodermis were the three dermal tissue domains studied in this work, with thicknesses of 0.05mm, 1.95mm, and 10mm, respectively, in a thin epidermis model. However, the epidermal layer tissue can be up to 1.5mm thick in certain places.[31] As a result, the model has an epidermal thickness of 1.5 mm, a dermis thickness of 1.5 mm, and a subcutaneous fat thickness of 9 mm. It is a symmetrical 2D model located around an axis. It will be a Bioheat-based model. A mathematical model was irradiated with a laser in this study, with the laser point being circular and the laser irradiating a perpendicular layer, as illustrated in Fig. 1. It also assumes that the tissues in the same tissue layer are homogenous, implying that thermal and optical characteristics do not change within the same tissue layer.

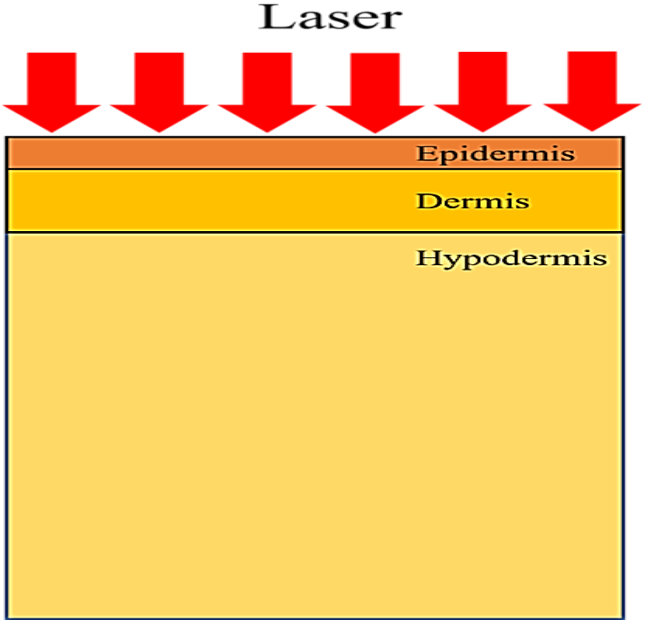

Fig. 1 Physical model.

2.2 Equation

2.2.1 Equation of heat transfer analysis

During the laser irradiation process, the interaction is a transient heat transfer calculated by a commercial program employing the finite-element method, a non-chemical reaction in the tissue, and an axially symmetrical 2D model in which each contact surface is smooth, and the characteristics of each tissue layer are identical within the same layer. It further specifies that all tissues be homogeneous and isotropic. The temperature distribution within each skin layer, as determined by Pennes' biological tissue heat transfer equation, may efficiently describe how heat transfer happens within the skin. This may be expressed as an Equation (1):

$$\rho C \frac{\partial T}{\partial t} = (k\nabla^2 T) + \rho_b C_b w_b (T_b - T) + Q_{ext} + Q_{met} \quad (1)$$

where, ρ is density of tissue [kg/m^3], C is tissue heat capacity [J/kg°C], k is tissue thermal conductivity [W/m.°C], T is temperature of tissue [°C], $T_b$is blood temperature [°C], $\rho_b$is blood density [kg/m^3], C_b is blood specific heat capacity [J/kg °C], $w_b$is blood perfusion rate [1/s], Q_{met} is a source of metabolic heat [W/m^2], Q_{ext} is an external source of heat [W/m^2]. In this study Q_{ext} is thermal energy generated by the laser. and $\rho_b C_b w_b (T_b - T)$ is the term caused by the diffusion of blood within the tissues.

2.2.2 Boundary conditions

Figures 2 and 3 show the boundary conditions and physical characteristics of the model domain where external thermal energy is estimated using Beer-lambert's Law and Light transport equation. A condition is the top surface of the layer (z = 0). The convection boundary is shown in Equation (2).

$$-n(-k\nabla T) = h_{am}(T - T_{am}) \quad (2)$$

where T_{am} is temperature in the environment [°C], h_{am} is air coefficient of convection [W/m^2.K], except for the upper surface, the outer surface of the tissue layer maintains the body's core temperature. (T_c) as an adiabatic boundary condition. The three internal layers have no contact resistance, it is assumed, which is considered a continuity boundary condition. Shown as shown in Equation (3).

$$n \cdot (k_u \nabla T_u - k_d \nabla T_d) = 0 \quad (3)$$

In this study, when considering laser beam irradiation in boundary conditions, the thermal energy generated by a laser can be described by equations according to Beer Lambert's Law and Light Transport Equation, with the following equations.

The laser irradiation of the model's top surface at a depth of the laser radiation intensity is described by Beer Lambert's Law as Equation (4).

$$I(z) = I_0 e^{(-r^2/2\sigma^2)} \cdot e^{bz} \cdot e^{-(a+b)z} \quad (4)$$

when I_0 is the intensity of laser radiation absorbed by the skin [W/mm^2], a is tissue absorption coefficient [1/m], b is tissue scattering coefficient [1/m], z is a tissue depth [mm], and σ is the radius of the laser beam in a laser irradiation [mm]. Therefore, the thermal energy of laser irradiation according to Beer Lambert's Law is expressed as Equation (5).

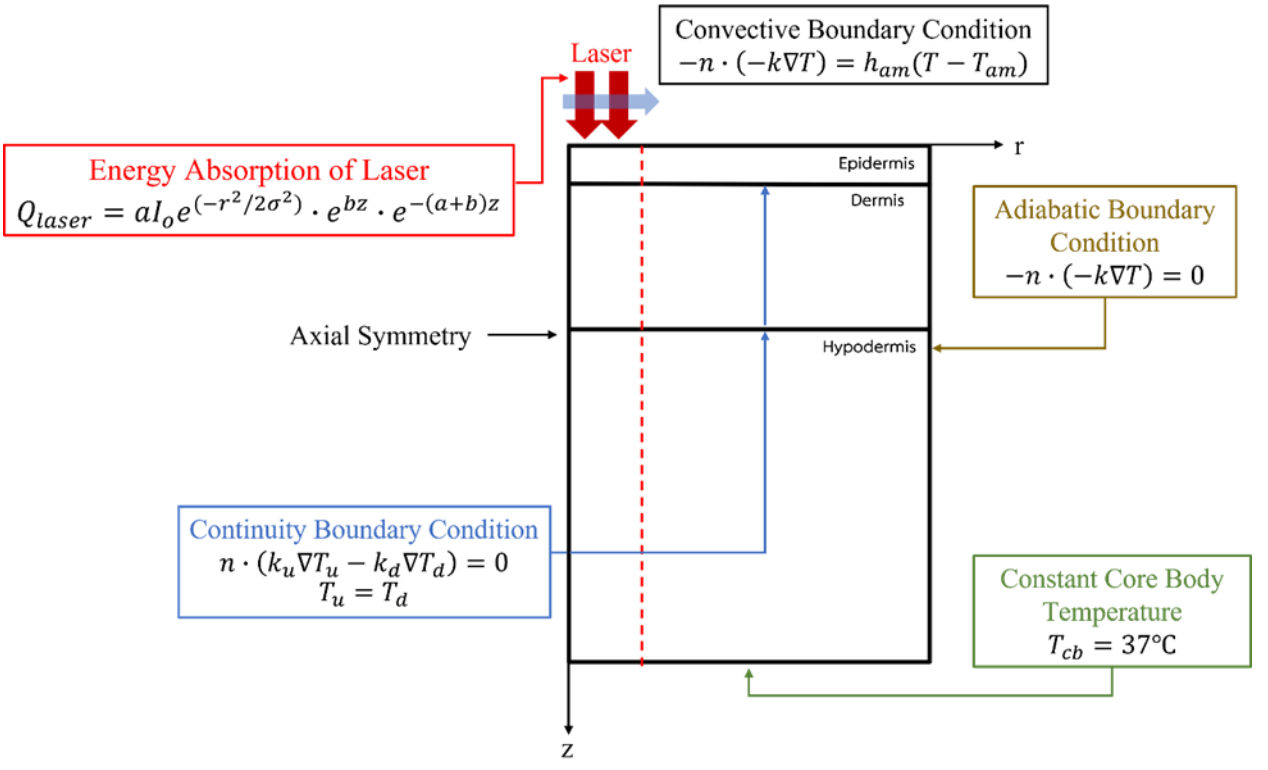

Fig. 2 Boundary conditions of beer lambert's law.

$$Q_{laser,b} = a \cdot I_0 e^{(-r^2/2\sigma^2)} \cdot e^{bz} \cdot e^{-(a+b)z} \quad (5)$$

The thermal energy of the laser is called the Light Transport Equation in Equation (6), and the diffusion coefficient is calculated in Equation (7). After that, the thermal energy of the laser is calculated in Equation (8).

$$\frac{\partial \emptyset}{\partial t} - D\nabla^2 \emptyset + c_* \mu_a \emptyset = 0 \quad (6)$$

$$D = c_*[3(\mu_a + (1-g)\mu_s)]^{-1} \quad (7)$$

$$Q_{laser,l} = \mu_a \emptyset \quad (8)$$

when $\emptyset$ is thermal energy per volume unit [W/m^2], c_* is speed of light in tissue components [m/s], μ_a is absorption coefficient of tissue [1/m], μ_s is scattering coefficient of tissue [1/m], and g is the optical property values in each medium indicate the diffusion direction. However, when studying the physical properties of light, taking into consideration the reflection of light in each wavelength, the intensity of laser radiation absorbed by the skin varies, as indicated in Equation (9).

$$\emptyset = (1-r) \cdot \emptyset_0 \cdot e^{(-r^2/2\sigma^2)} \quad (9)$$

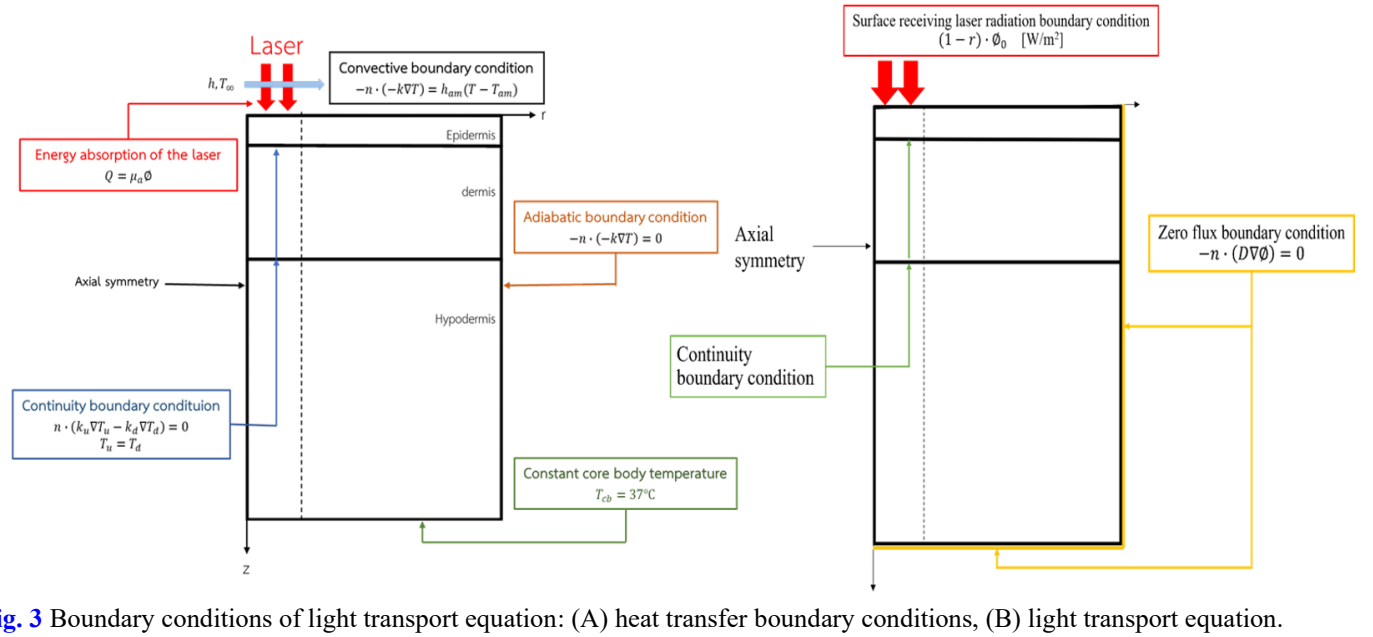

Fig. 3 Boundary conditions of light transport equation: (A) heat transfer boundary conditions, (B) light transport equation.

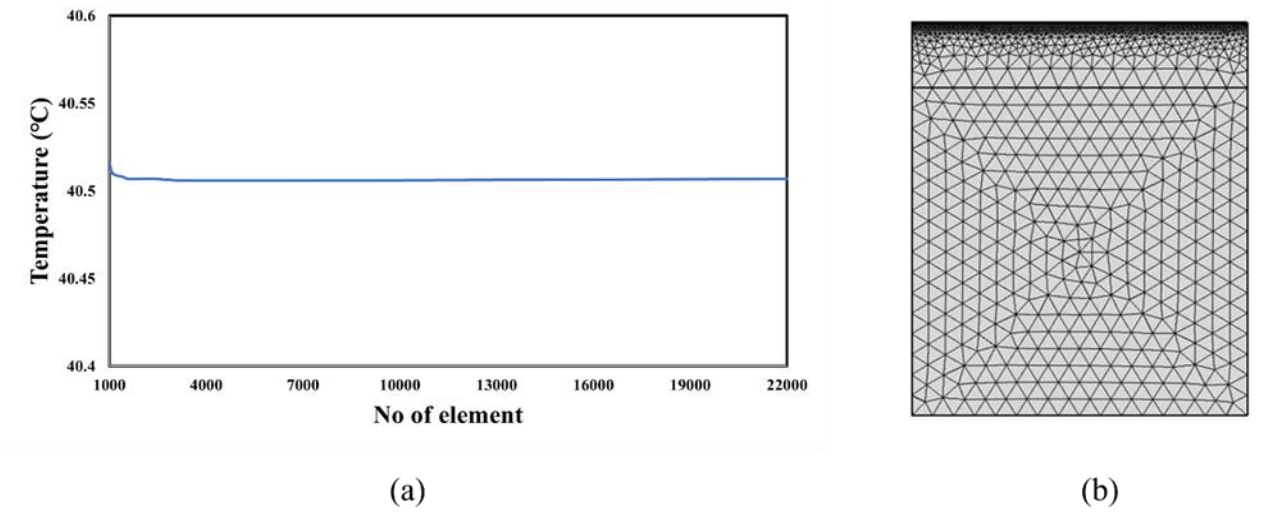

Fig. 4 Meshing: (a) Mesh independent, (b) Mesh model.

In the lower and upper lateral regions, the areas that are not irradiated by the laser do not receive direct flux from the laser, shown in Equation (10)

$$-n \cdot (D\nabla\emptyset) = 0 \quad (10)$$

The epidermis and dermis absorption and scattering coefficients were calculated from the theory of Jacques.[32] The total epidermis absorption coefficient is affected by skin absorption $\mu_a$epi at the basal line slightly and the absorption of melanin is outstanding because of the melanosomes in the epidermis, the wavelength independent parameters (nm) and melanosome volume fraction (f.mel) (Fig. 4). The $\mu_a$epi can be specified in units of cm^{-1}.

The baseline absorption coefficient of the insignificant epidermis ($\mu_a skin.bl$)

The following equations are used to determine the epidermis and dermis baseline absorption $\mu_a skin.bl$ is expressed as a function of the wavelength (nm), as in equation (11).

$$\mu_a skin.bl = 0.244 + 85.3e^{\frac{-(nm-154)}{66.2}} \ [\text{cm}^{-1}] \quad (11)$$

A single melanosome's absorption coefficient ($\mu_a mel$)

Melanin absorption often dominates epidermis absorption. Melanin is a polymer that results from the condensation of tyrosine molecules that has a broad absorbance range in most persons, which absorbs more strongly at shorter wavelengths. Melanin is found in melanosomes, which are membrane particles 1-2 micrometers in diameter, whose inner membrane is lined with many melanin granules about 10 nanometers on average melanin synthesis areas. There is an absorption coefficient, $\mu_a mel$, within the melanosome that is nearly the size and wavelength dependence (nm), as shown in Equation (12).

$$\mu_a mel = (6.6 \times 10^{11})(nm^{-3.33}) \ [\text{cm}^{-1}] \quad (12)$$

The melanosome volume fraction in the epidermis

The percentage of epidermis volume occupied by the melanosome is used to calculate the estimated concentration range (Vf.mel). In this study, a moderately pigmented adult with a melanosome volume fraction of 10%.

Net epidermal absorption coefficient

$$\mu_a epi = (Vf.mel)(\mu_a mel) + (1 - Vf.mel)(\mu_a skin.bl)[\text{cm}^{-1}] \quad (13)$$

Scattering coefficient of the epidermis

Decreased scattering of the $\mu_s derm$ from the combined raven owing to Rayleigh and Mie scattering by large cylindrical cutaneous collagen fibers by microstructures involving collagen fibers and structures of other cells, the epidermis has keratin fibers that appear like dermis, and $\mu_s epi$ is essentially $\mu_s Mie.fiber$ fiber scattering from Mie's theory given by Equation (14).

$$\mu_s Mie.fiber = (2 \times 10^5)(nm^{-1.5}) \ [\text{cm}^{-1}] \quad (14)$$

Rayleigh scattering by microstructures involving collagen fibers and other cellular structures.

$$\mu_s Rayleigh = (2 \times 10^{12})(nm^{-4}) \ [\text{cm}^{-1}] \quad (15)$$

Total scattering,

$$\mu_s = \mu_s Mie.fiber + \mu_s Rayleigh \quad (16)$$

Dermal absorption coefficient when perfused with blood.

The optical absorption of the true dermis depends on the amount of blood it contains. Specify the mean assuming that the blood is a volumetric fraction that is evenly spread throughout the skin. The volume fraction in this area tends to be about 2-5% by tissue. Other areas of the dermis, $f.blood$

in that area is significantly less. The dermis's net absorption is calculated from Equation (17).

$$\mu_a dem = (f.blood)(\mu_a blood) + (1 - f.blood)(\mu_a skin.bl) \quad (17)$$

Blood absorption at 45% hematocrit is obtained from Equation (18).

$$\mu_a blood = S\mu_{a.oxy} + (1 - S)\mu_{a.deoxy} \quad (18)$$

$\mu_{a.oxy}$ and $\mu_{a.deoxy}$ take data from[33]

3. Method

In this study, a mathematical model of a multilayer tissue irradiated with a laser was developed. This model was modified by the FEM method to analyze the light transport equations and their respective boundary conditions in the 2D axial symmetry problem. This phenomenon is dependent on variable parameters including wavelength, laser beam radius, laser intensity, and tissue layer thickness. To investigate a valid and precise thermal mathematical model, we validated our model with previous research. The model was evaluated using the FEM method. The model has been divided into triangular elements. We examined the element sizes for suitability for the study with precision and brevity. The triangular element parsing model was a convergence test at a wavelength of 694 nm, a laser beam diameter of 2 mm at a flow rate of 50 J/cm^2. The process of obtaining the desired results begins with the input of parameters such as thermal and optical properties, and then the bio-thermal energy is calculated using laser thermal energy derived from the temperature distribution.

Figure 5 shows the procedure. To acquire a temperature distribution, the thermal and optical properties shown in Table 2 are applied to time-dependent solutions to investigate convergence.

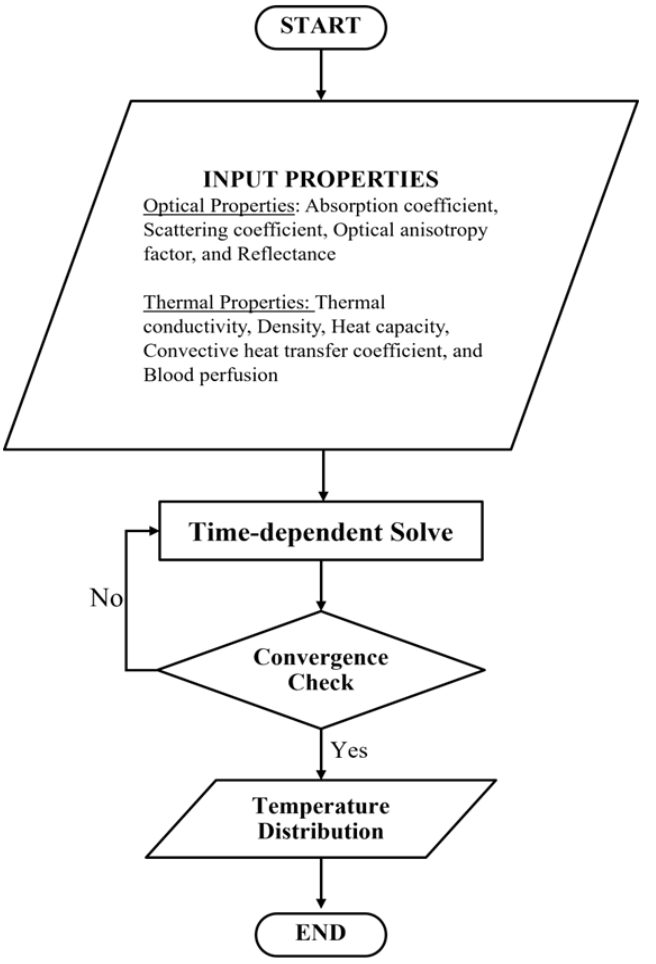

Fig. 5 depicts the stages of the calculation procedure.

4. Result and discussion

4.1 Model verification

Compare previous research that has been tested to validate the validity of models used to investigate laser-thermal bio-models where the laser-thermal energy is obtained from two equations as (5) and (8), respectively.

Previous study with Wongchadakul *et al*., studies. The heat transfer properties of the skin produced by lasers are investigated in this work. Using laser irradiation energy absorption specified by the bio-tissue heat transfer equation and Beer Lambert's law, the temperature fluctuations of the epidermal layers were investigated. To ensure the accuracy of the work done by comparing the temperature of the 2D model with axial symmetry at an 800 nm wavelength, the 2 W/mm^2 laser radiation intensity at 600 s, as shown in Fig. 6.

Zhang *et al*. investigated the Estimation of Diffusion and Monte Carlo models for Light dispersion simulated multilayered human skin, with or without blood vessels. Fig. 7 shows the thermal energy from the laser estimated using the Light Transport Equation, which is used to validate the biological model by comparing the model's surface temperature.

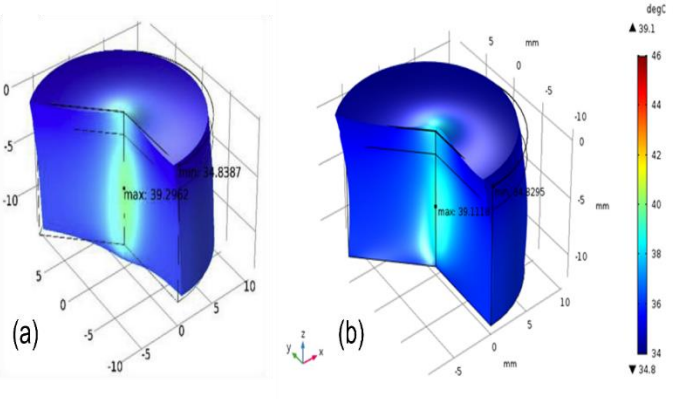

Fig. 6 Comparing skin temperature distribution: (a) previous studies, (b) present studies.

4.2 Distribution of Temperature

This study looked at temperature distribution differences in

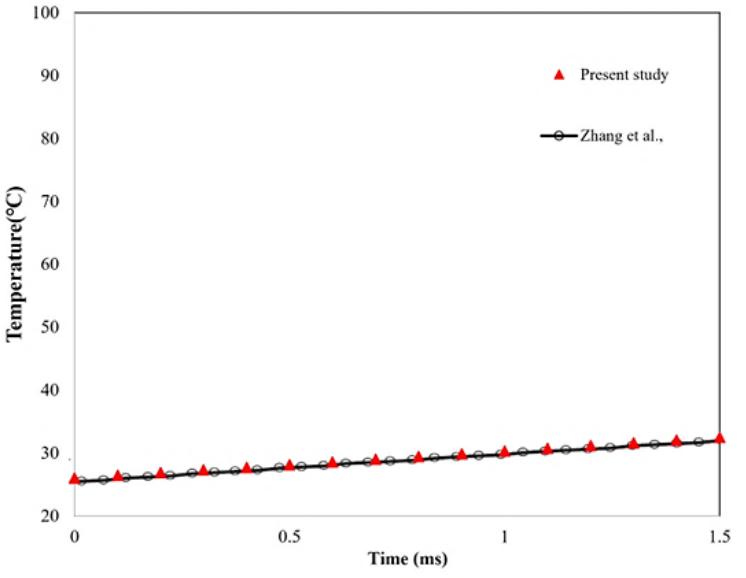

Fig. 7 Comparing skin temperature over 1.5 ms of Zhang studies and present studies.

biological models of 3 tissue layers (epidermis, dermis, and hypodermis). The external thermal energy was calculated using two equations, Beer Lambert's law and the Light Transport Equation, for a total of three laser wavelengths, 698 nm, 800 nm, and 980 nm, with a fluent rate of 50 J/cm^2 laser radiation, and 100 J/cm^2 laser radiation, and laser beam radius of 1 mm and 2 mm, respectively.

Figures 8(a-d) demonstrates the temperature distribution in the model at 694 nm, with the majority of the temperature occurring at the upper surface due to the limited penetrating power of short-wavelength lasers. As a result, most of the energy is deposited on the upper surface, where it becomes temperature. The temperature distributions of the two computational laser models are comparable. Since the light transport equation is determined, the model that calculates laser power using the optical transport equation has a high temperature dispersion in a depth and width of approximately 2-3 mm, as shown in Fig. 9. In the model, the propagation of the transmitted light reveals the behavior of the incident light, whether it be the direction of refraction or reflection. However, Beer-Lambert's law is an approximation of the depth, exponential width, and depth attenuation of energy. As depicted in Figs. 8(e–l), the elevated temperature in the deep layer is evident in the light transport equation model at the 800 nm wavelength when using lasers at both 800 nm and 980 nm. This is evident in Fig. 8(e), which depicts the distribution of temperature in the hypodermis. Light may not propagate through the deep layers of both models if the epidermis is thicker than 1.5 mm. However, if the epidermis is only 0.05 mm thick, there is a significant difference between the two models. Therefore, the characteristics of the temperature distribution are comparable to those of laser irradiation with a wavelength of 694 nm.

When the epidermis layer thickness is increased to 1.5 mm, the resulting heat is retained in the epidermis layer due to the transmission and absorption of laser light by the epidermis layer. The light transport equation and Beer-Lambert's law both predicted that the epidermis would absorb energy. The maximum temperature generated by the models varied substantially with increasing epidermal thickness for each laser wavelength. Figs. 8(a-d) demonstrates that in low-wavelength lasers, laser energy is more concentrated in the epidermis than in high-wavelength lasers. At wavelength 694, the temperature is distributed throughout the epidermis, and its maximal temperature is greater than that of laser models with wavelengths of 800 nm and 980 nm, according to Beer-Lambert's Law and the Light Transport Equation.

Figure 9 depicts the temperature at the model's core depth and the radial upper surface temperature depicted in Fig. 8(e). At a depth of approximately 2 to 3 mm, the temperature difference resulting from the laser-powered simulation of Beer-Lambert's law and the light transport equation is plainly visible. As the wavelength of the laser radiation increases, so does its penetrability. However, the temperature behavior predicted by Beer-Lambert's law differs from that predicted by Beer-Lambert's model, which is an estimate of the thermal energy decrease along the depth and in the radius. However, the model based on the light transport equation analyzes and estimates the behavior of currying in the medium.

Comparison with models of epidermis with different thickness is shown in Fig. 10 where (A) is a model with epidermis thickness of 1.5 mm and (B) is a model with

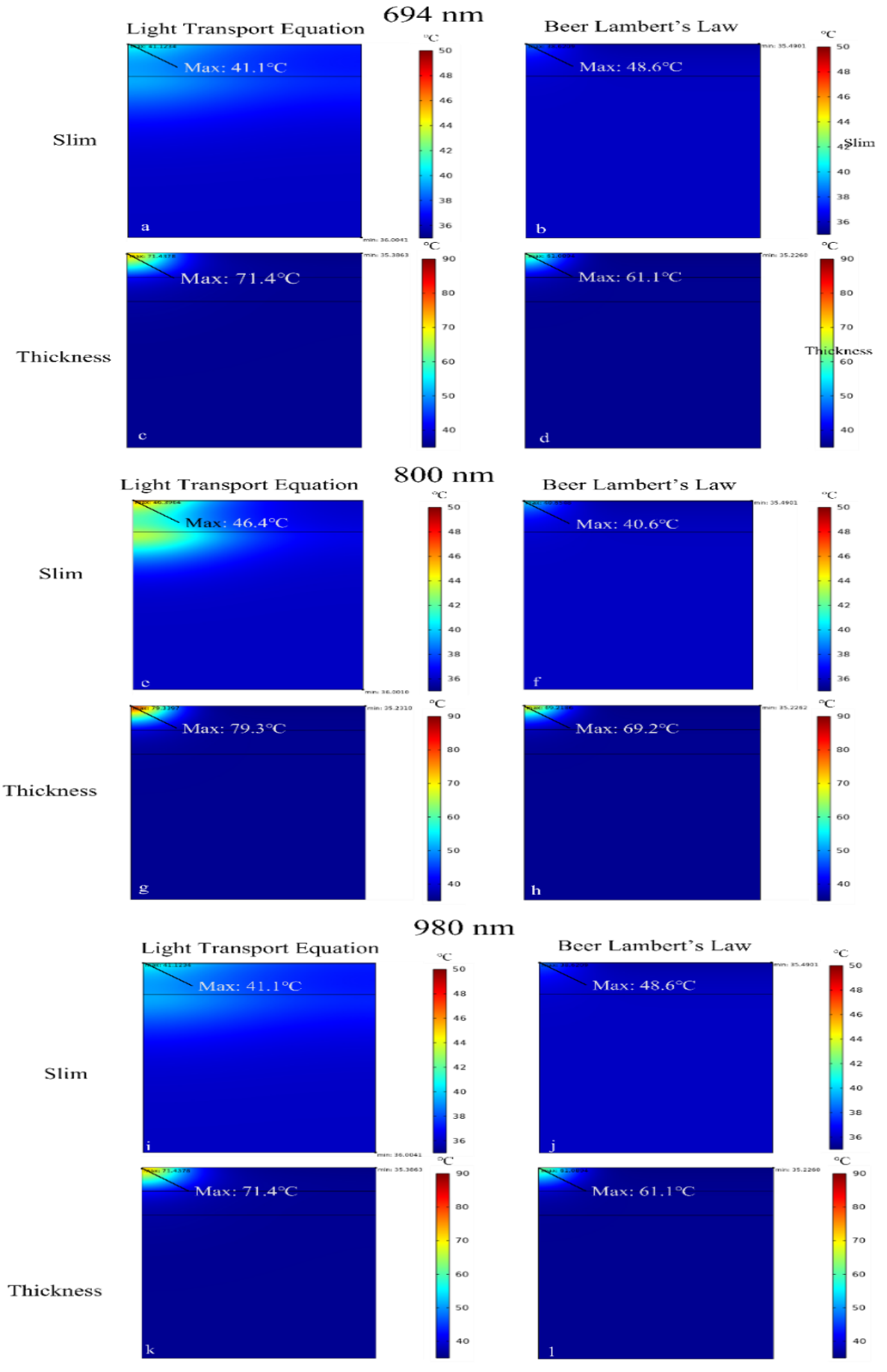

Fig. 8 Temperature Distribution of wavelength 694 nm, 800 nm and 980 am at 1 mm radius of laser at 10 sec.

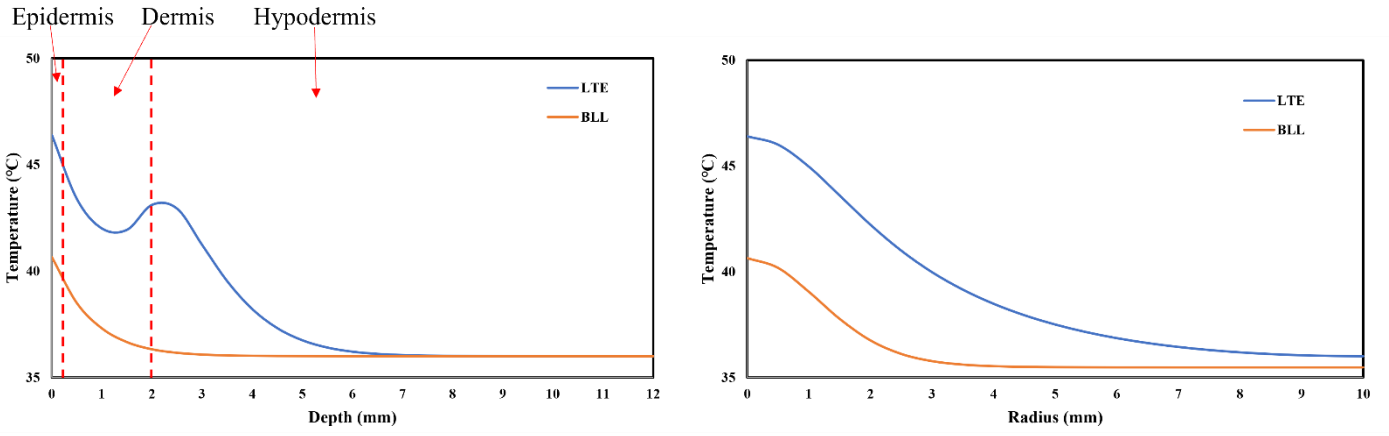

Fig. 9 Comparison of temperature distribution from laser irradiation between Beer Lambert's law and Light Transport Equation at 800 nm, radius of laser 1 mm, and 50 J/cm^2.

epidermis thickness of 0.05 mm. The models used each equation to calculate the heat energy when the thickness of the epidermis was raised from 0.05 mm to 1.5 mm. The temperatures for models using Beer-lambert's law and Light transport equation were similar. But the Light transport equation model had a peak temperature 6-10 °C higher than Beer-lambert's law, depending on the laser wavelength. Because the Light transport equation model approximates the behavior of the generated light, it has a higher temperature distribution than Beer-lambert's law.

In addition, Beer-Lambert's law, and the light transport equation act similarly in the epidermis model with a thickness of 1.5 mm. As the epidermis has a high absorption coefficient, the laser energy reaching the deeper layer decreases as the epidermis layer becomes thicker in both models. If it is necessary to treat a region with a thick epidermis, it may be necessary to account for heat accumulation in the epidermis if the region to be treated is located deep in the dermis or hypodermis.

As shown in Figs. 11(a-d), when the radius of the laser beam was extended to 2 mm, the top surface region of the model received higher energy, larger radial temperature distribution, but a little increase in temperature in the deep layer. There was a little difference in the low wavelength model at roughly 8°C between the models using Beer-lambert's law and Light transport equation. However, there was a notable difference. in temperature distribution in the depth of the model when using the higher laser wavelengths, as shown in Figs. 11(e-l), which are 800 and 980 nm, respectively. If the laser beam was increased in the model with a 1.5 mm thick epidermis, the temperature distribution remained in the epidermis area. It is possible that increasing the laser beam radius had little influence on temperature profile in the depth layer in both the Beer-lambert's law and Light transport equation models.

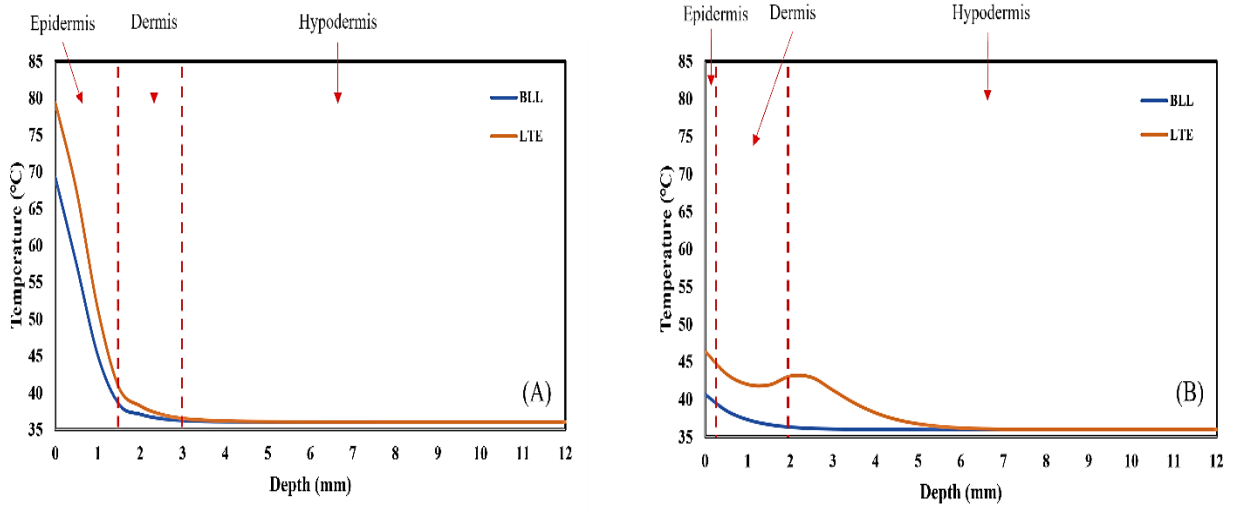

Fig. 10 Compare between the (A)Thickness epidermis model and (B) slim epidermis model at 800 nm laser wavelength with 50 J/cm^2 and 1 mm laser beam radius.

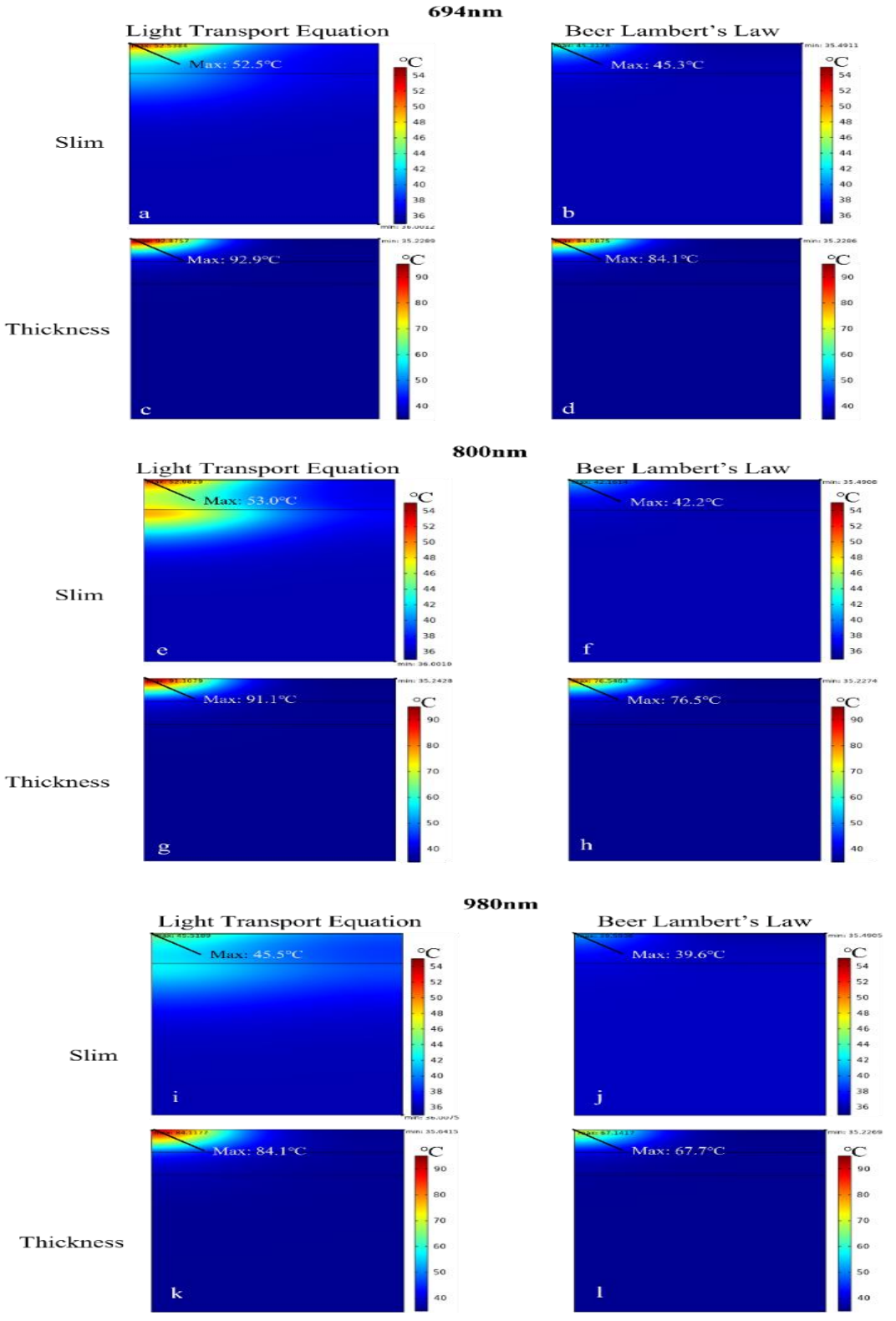

Fig. 11 Temperature Distribution of wavelength 694 nm, 800 nm and 980 am at 2 mm radius of laser at 10 sec.

Figure 12 shows that when we irradiate a laser with a higher fluent rate, an increase in the temperature distribution in the depth layer is evident in a model where the laser energy is calculated from Light transport equation. Most of the temperature in the Beer-lambert's law model accumulates in the upper layer of the model as energy depletion throughout the depths, but in the Light transport equation model, the physical qualities of the light are transmitted into the model. As shown in Figs. 12(e-l), the temperature distribution of the two model equations was similar in the model treated with lasers with a short wavelength of 694.

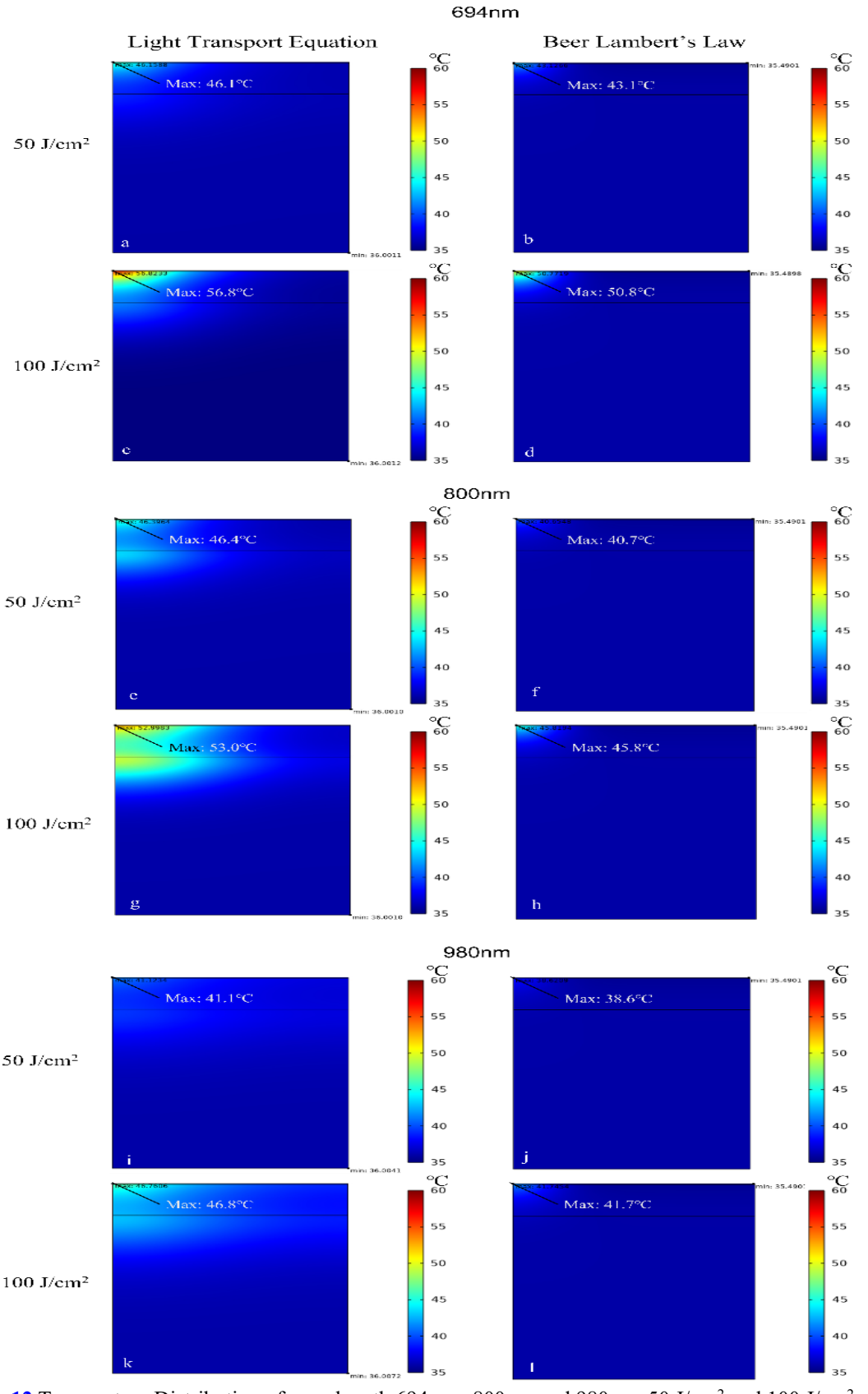

Fig. 12 Temperature Distribution of wavelength 694 nm, 800nm and 980nm, 50 J/cm^2 and 100 J/cm^2 at 10 sec.

5. Conclusion

In this study, a mathematical model for the pre-diagnosis of laser thermal therapy that calculates the laser heat energy from two equations was studied: Beer Lambert's Law and Light Transport Equation, is used to estimate the difference in thermal energy. The temperature distribution was studied in a

model irradiated with 3 wavelengths of laser at 694 nm, 800 nm, and 980 nm with 1mm and 2mm laser beam radius by laser irradiation with laser radiation intensity at 50 J/cm^2 and 100 J/cm^2 within 10 seconds.

The light transport equation model has a more pronounced temperature distribution depth when laser-irradiated at longer wavelengths than when laser-irradiated at lower wavelengths since light at higher wavelengths penetrates more deeply. The light transport equation model has a greater temperature distribution in depth and width than Beer-Lambert's Law because the light transport equation corresponds to the behavior of light within the tissue. However, they are comparable at shorter wavelengths. Additionally, if the epidermis layer is dense, energy will accumulate, resulting in a high temperature.

Because the physical characteristics of the tissue are porous, consisting of a solid phase (tissue) and a liquid phase (blood), this study can be used to enhance the porosity of the model in future research. which will be closer to the actual characteristics of the tissue**.** The tumor domain may be added to the model to examine the temperature distribution within the tumor and the temperature occurring in healthy tissue to ascertain the extent of the lesions' practicable treatment.

Acknowledgements

This work was supported by the Thailand Science Research and Innovation Fundamental Fund fiscal year 2023 (Contract No. TUFF180228/2566) and (TUFF41/2566), special thanks to National Research Council of Thailand (NRCT) (Contact no. N42A650197), Graduate Studies Faculty of Engineering, Thammasat School of Engineering, Thammasat University, Thammasat University Research Fund Contract No. TUFT 19/2565.

References

[1] T. H. Maiman, Stimulated optical radiation in ruby, *Nature*, 1960, **187**, 493-494, doi: 10.1038/187493a0.

[2] Q. Peng, A. Juzeniene, J. Chen, L. O. Svaasand, T. Warloe, K.-E. Giercksky, J. Moan, Lasers in medicine, *Reports on Progress in Physics*, 2008, **71**, 056701, doi: 10.1088/0034-4885/71/5/056701.

[3] M. J. C. van Gemert, A. J. Welch, Clinical use of laser-tissue interactions, *IEEE Engineering in Medicine and Biology Magazine*, 1989, **8**, 10-13, doi: 10.1109/51.45950.

[4] J. Wilkin, M. Dahl, M. Detmar, L. Drake, A. Feinstein, R. Odom, F. Powell, Standard classification of rosacea: report of the national rosacea society expert committee on the classification and staging of rosacea, *Journal of the American Academy of Dermatology*, 2002, **46**, 584-587, doi: 10.1067/mjd.2002.120625.

[5] J. Lepselter, M. Elman, Biological and clinical aspects in laser hair removal, *Journal of Dermatological Treatment*, 2004, **15**, 72-83, doi: 10.1080/09546630310023152.

[6] L. Andreassi, UV exposure as a risk factor for skin cancer, *Expert Review of Dermatology*, 2011, **6**, 445-454, doi: 10.1586/edm.11.54.

[7] U. Leiter, U. Keim, C. Garbe, Epidemiology of skin cancer: update 2019. Sunlight, Vitamin D and Skin Cancer, *Advances in Experimental Medicine and Biology*, Cham: Springer International Publishing, 2020: 123-139, doi: 10.1007/978-3-030-46227-7_6.

[8] S. Alaqeel, L. Alnaim, R. Abuzaid, R. AlSudairi, M. Hiligsmann, pcn473 preferences for chemotherapy side effects in Saudi breast cancer patients: a discrete-choice experiment, *Value in Health*, 2019, **22**, S528-S529, doi: 10.1016/j.jval.2019.09.665.

[9] D. Manstein, G. S. Herron, R. K. Sink, H. Tanner, R. R. Anderson, Fractional photothermolysis: A new concept for cutaneous remodeling using microscopic patterns of thermal injury, *Lasers in Surgery and Medicine*, 2004, **34**, 426-438, doi: 10.1002/lsm.20048.

[10] E. Y.-K. Ng, L. T. Chua, Prediction of skin burn injury. Part 2: Parametric and sensitivity analysis, Proceedings of the Institution of Mechanical Engineers, *Part H: Journal of Engineering in Medicine*, 2002, **216**, 171-183, doi: 10.1243/0954411021536388.

[11] H. H. Pennes, Analysis of tissue and arterial blood temperatures in the resting human forearm, *Journal of Applied Physiology*, 1948, **1**, 93-122, doi: 10.1152/jappl.1948.1.2.93.

[12] M. Jaunich, S. Raje, K. Kim, K. Mitra, Z. Guo, Bio-heat transfer analysis during short pulse laser irradiation of tissues, *International Journal of Heat and Mass Transfer*, 2008, **51**, 5511-5521, doi: 10.1016/j.ijheatmasstransfer.2008.04.033.

Megan, Jaunich, Bio-heat transfer analysis during short pulse laser irradiation of tissues, *International Journal of Heat and Mass Transfer*, 2008, **51**, 5511-5521, doi: 10.1016/j.ijheatmasstransfer.2008.04.033.

[13] A. Bhowmik, R. Repaka, S. C. Mishra, K. Mitra, Thermal assessment of ablation limit of subsurface tumor during focused ultrasound and laser heating, *Journal of Thermal Science and Engineering Applications*, 2016, **8**, 011012, doi: 10.1115/1.4030731.

[14] T.-H. Kim, G.-W. Lee, J.-I. Youn, A comparison of temperature profile depending on skin types for laser hair removal therapy, *Lasers in Medical Science*, 2014, **29**, 1829-1837, doi: 10.1007/s10103-014-1584-6.

[15] P. Wongchadakul, P. Rattanadecho, T. Wessapan, Implementation of a thermomechanical model to simulate laser heating in shrinkage tissue (effects of wavelength, laser irradiation intensity, and irradiation beam area), *International*

Journal of Thermal Sciences, 2018, **134**, 321-336, doi: 10.1016/j.ijthermalsci.2018.08.008.

[16] P. Wongchadakul, P. Rattanadecho, T. Wessapan, Simulation of temperature distribution in different human skin types exposed to laser irradiation with different wavelengths and laser irradiation intensities, *Songklanakarin Journal of Science and Technology*, 2019, 41 (3), 529-538.

[17] P. Wongchadakul, P. Rattanadecho, Mathematical modeling of multilayered skin with embedded tumor through combining laser ablation and nanoparticles: effects of laser beam area, wavelength, intensity, tumor absorption coefficient and its position, *International Journal of Heat and Technology*, 2021, **39**, 89-100, doi: 10.18280/ijht.390109.

[18] M. S. Patterson, B. Chance, B. C. Wilson, Time resolved reflectance and transmittance for the noninvasive measurement of tissue optical properties, *Applied Optics*, 1989, **28**, 2331, doi: 10.1364/ao.28.002331.

[19] G. Shafirstein, W. Bäumler, M. Lapidoth, S. Ferguson, P. E. North, M. Waner, A new mathematical approach to the diffusion approximation theory for selective photothermolysis modeling and its implication in laser treatment of port-wine stains, *Lasers in Surgery and Medicine*, 2004, **34**, 335-347, doi: 10.1002/lsm.20028.

[20] R. Zhang, W. Verkruysse, G. Aguilar, J. Stuart Nelson, Comparison of diffusion approximation and Monte Carlo based finite element models for simulating thermal responses to laser irradiation in discrete vessels, *Physics in Medicine and Biology*, 2005, **50**, 4075-4086, doi: 10.1088/0031-9155/50/17/011.

[21] A. Paul, A. Paul, Thermo-mechanical assessment of nanoparticle mixed vascular tissues under pulsed ultrasound and laser heating, *International Journal of Thermal Sciences*, 2021, **163**, 106815, doi: 10.1016/j.ijthermalsci.2020.106815.

[22] V. Mongkol, W. Preechaphonkul, P. Rattanadecho, Photo-thermo-mechanical model for laser hair removal simulation using multiphysics coupling of light transport, heat transfer, and mechanical deformation (case study), *Case Studies in Thermal Engineering*, 2023, **41**, 102562, doi: 10.1016/j.csite.2022.102562.

[23] F. Ebrahimi, E. Salari, Thermal loading effects on electro-mechanical vibration behavior of piezoelectrically actuated inhomogeneous size-dependent Timoshenko nanobeams, *Advances in Nano Research*, 2016, **4**, 197-228, doi: 10.12989/anr.2016.4.3.197.

[24] E. Salari, S. A. Sadough Vanini, Nonlocal nonlinear static/dynamic snap-through buckling and vibration of thermally post-buckled imperfect functionally graded circular nanoplates, *Waves in Random and Complex Media*, 2022, 1-47, doi: 10.1080/17455030.2022.2055810.

[25] E. Salari, A. R. Ashoori, S. A. sadough vanini, Porosity-dependent asymmetric thermal buckling of inhomogeneous annular nanoplates resting on elastic substrate. *Advances in Nano Research*, 2018, **7**, 25-38, doi: 10.12989/anr.2019.7.1.025.

[26] F. Ebrahimi, E. Salari, Semi-analytical vibration analysis of functionally graded size-dependent nanobeams with various boundary conditions, *Smart Structures and Systems*, 2017, **19**, 243-257, doi: 10.12989/sss.2017.19.3.243.

[27] F. Ebrahimi, E. Salari, Effect of non-uniform temperature distributions on nonlocal vibration and buckling of inhomogeneous size-dependent beams. Advances in Nano Research, 2018, **6**, 377-397, doi: 10.12989/anr.2018.6.4.377.

[28] A. R. Ashoori, S. A. S. Vanini, E. Salari, Size-dependent axisymmetric vibration of functionally graded circular plates in bifurcation/limit point instability, *Applied Physics A*, 2017, **123**, 1-14, doi: 10.1007/s00339-017-0825-5.

[29] E. Salari, A. R. Ashoori, S. A. Sadough Vanini, A. H. Akbarzadeh, Nonlinear dynamic buckling and vibration of thermally post-buckled temperature-dependent FG porous nanobeams based on the nonlocal theory, *Physica Scripta*, 2022, **97**, 085216, doi: 10.1088/1402-4896/ac8187.

[30] E. Salari, S. Ali Sadough Vanini, A. Ashoori, Nonlinear thermal stability and snap-through buckling of temperature-dependent geometrically imperfect graded nanobeams on nonlinear elastic foundation, *Materials Research Express*, 2020, **6**, 1250j6, doi: 10.1088/2053-1591/ab5e50.

[31] Tasneem Poonawalla and Dayna Diven, Anatomy of the Skin, 2008, Available from: https://www.utmb.edu/pedi_ed/CoreV2/Dermatology/page_03.htm.

[32] S. L. Jacques, Skin Optics, *Oregon Medical Laser Center News*, 1998, Available from: https://omlc.org/news/jan98/skinoptics.html.

[33] S. Wray, M. Cope, D. T. Delpy, J. S. Wyatt, E. O. R. Reynolds, Characterization of the near infrared absorption spectra of cytochrome aa3 and haemoglobin for the non-invasive monitoring of cerebral oxygenation, *Biochimica et Biophysica Acta (BBA) - Bioenergetics*, 1988, **933**, 184-192, doi: 10.1016/0005-2728(88)90069-2.

[34] G. Aguilar, S. H. Díaz, E. J. Lavernia, J. Stuart Nelson, Cryogen spray cooling efficiency: improvement of port wine stain laser therapy through multiple-intermittent cryogen spurts and laser pulses, *Lasers in Surgery and Medicine*, 2002, **31**, 27-35, doi: 10.1002/lsm.10076.

[35] F. Xu, T. Wen, K. Seffen, T. Lu, Modeling of skin thermal pain: a preliminary study, *Applied Mathematics and Computation*, 2008, **205**, 37-46, doi: 10.1016/j.amc.2008.05.045.

